SINGLE IMAGE HAZE REMOVAL VIA A SIMPLIFIED DARK CHANNEL

Zhengguo Li, Jinghong Zheng, Wei Yao, and Zijian Zhu

Signal Processing Department, Institute for Infocomm Research, 1 Fusionopolis Way, Singapore

ABSTRACT

Images of outdoor scenes could be degraded by haze, fog, and smoke in the atmosphere. In this paper, we propose a novel single image haze removal algorithm by introducing a minimal color channel and a sky region compensation term. A simplified dark channel is computed via the minimal color channel. The transmission map is first estimated by using the simplified dark channel. To avoid amplifying noise in the sky, a non-negative sky region compensation term is proposed to adjust the transmission map in the sky. The map is then refined via a content adaptive guided image filter and is finally applied to recover the haze image. Experimental results on outdoor images with haze and without haze demonstrate that the proposed algorithm outperforms existing algorithms.

1. INTRODUCTION

Images of outdoor scenes often suffer from bad weather conditions such as haze, fog, smoke and so on. The light is scattered and absorbed by the aerosols in the atmosphere, and it is also blended with airlight reflected from other directions. This process fades the color and reduces the contrast of captured objects, and the degraded images often lack visual vividness. Therefore, haze removal is highly demanded in image processing, computational photography and computer vision applications [1].

It is very challenging to remove haze from hazed images because the haze depends on unknown depth information, especially when there is only a single haze image. This is because the haze removal problem is under-constrained in this case. Many methods were presented by using multiple images or additional information [2, 3, 4]. For example, haze is removed by using a polarization based method in [3] through two or more images taken with different degrees of polarization. Depth information either from user inputs or from 3D models is required by a depth based method in [4]. Unfortunately, applications of the methods are limited because of their requirements on the inputs. Recently, haze removal via single image attracted much interest and made significant progresses. A single image haze removal algorithm was proposed in [5] by maximizing the local contrast of the restored image. The results are visually compelling while they might not be physically valid. The algorithm proposed by Fattal [6] is sound reasonable from the physical point of view and it can also produce impressive results. However, this algorithm could fail in presence of heavy haze. An interesting dark channel prior based single image haze removal algorithm was proposed in [7]. The dark channel prior is based on an observation of haze-free outdoor images, i.e., in most of the local regions which do not cover the sky, it is very often that some pixels have very low intensity in at least one color (RGB) channel. The algorithm is physically valid and can handle distant objects even in images with heavy haze. However, noise in the sky could be amplified and color in brightest regions could be distorted by using the algorithm in [7] even though a lower bound was introduced for the transmission map in [7]. It is thus desired to design a new single image haze removal algorithm to avoid those problems mentioned above.

In this paper, a new single image haze removal algorithm is proposed by introducing a minimal color channel and a sky region compensation term. The minimal color channel of a pixel is defined as the minimal value among all color components of the pixel. A simplified dark channel is computed by using the minimal color channel. The initial value of the transmission map is estimated by using the simplified dark channel. The computational cost of the new estimation method is lower than the cost of the method in [7]. To avoid amplifying noise in the sky, a non-negative sky region compensation term is proposed to constrain the initial value of the transmission map in the sky. The map is then refined via a content adaptive guided image filter (GIF) [11] and is finally used to recover the haze image. The new haze removal algorithm can avoid/reduce halo artifacts, noise in the sky, and color distortion from appearing in the dehazed image. In addition, a very small amount of haze is left for the distant objects by the proposed haze removal algorithm. As a result, the feeling of depth in the dehazed image could be preserved better [15, 16]. Experimental results show that the algorithm is applicable to both images with haze and images without haze.

The rest of this paper is organized as follows. Existing works on GIFs are summarized in Section 2. Section 3 includes details on the proposed haze removal algorithm. Extensive experimental results are given in Section 4 to illustrate the efficiency of the proposed algorithm. Concluding remarks are provided in Section 5.

2. RELATED WORKS ON GUIDED IMAGE FILTERS

After estimating the transmission map via a dark channel prior, the value of the transmission map can be refined by using a GIF [8] or a content adaptive GIF [11]. In this section, both the GIF and the content adaptive GIF are summarized such that it is easy to follow the proposed single image haze removal algorithm.

In the GIF, a guidance image G is used which could be identical to the image X to be filtered. Let $\Omega_{\zeta_1}(p)$ be a square window centered at a pixel p of a radius ζ_1. It is assumed that the output image Z is a linear transform of the guidance image G in the window $\Omega_{\zeta_1}(p')$ [18, 19, 20]

$$Z(p) = a_{p'}G(p) + b_{p'}, \forall p \in \Omega_{\zeta_1}(p'), \tag{1}$$

where $a_{p'}$ and $b_{p'}$ are two constants in the window $\Omega_{\zeta_1}(p')$. Their values are obtained by minimizing a cost function $E(a_{p'}, b_{p'})$ which is defined as

$$E = \sum_{p \in \Omega_{\zeta_1}(p')} [(a_{p'} G(p) + b_{p'} - X(p))^2 + \lambda a_{p'}^2], \quad (2)$$

where λ is a regularization parameter penalizing large $a_{p'}$.

The GIF is one of the fastest edge-preserving local filters and it outperforms the bilateral filter [9] in the sense that the GIF can avoid gradient reversal artifacts. However, the value of λ in the GIF [8] is fixed. As such, halos are unavoidable for the GIF in [8] when it is forced to smooth edges. A content adaptive GIF was proposed in [11] to overcome the problem. The cost function in Equation (2) is replaced by the following one:

$$E = \sum_{p \in \Omega_{\zeta_1}(p')} [(a_{p'} G(p) + b_{p'} - X(p))^2 + \frac{\lambda}{\Gamma_G(p')} a_{p'}^2], \quad (3)$$

where $\Gamma_G(p')$ is an edge aware weighting and it is defined by using local variances of 3×3 windows of all pixels as follows [10]:

$$\Gamma_G(p') = \frac{1}{N} \sum_{p=1}^{N} \frac{\sigma_{G,1}^2(p') + \varepsilon}{\sigma_{G,1}^2(p) + \varepsilon}, \quad (4)$$

$\sigma_{G,1}^2(p')$ is the variance of G in the window $\Omega_1(p')$. ε is a small constant and its value is selected as $(0.001 \times L)^2$ while L is the dynamic range of the input image. Due to the box filter in [8], the complexity of $\Gamma_G(p')$ is $O(N)$ for an image with N pixels.

Due to the linear model in Equation (1), both the GIF and the content adaptive GIF can transfer structure from the guidance image G to the output image $\hat{Z}$ regardless of the smoothness of the image X to be filtered. Both filters can thus be applied to refine the transmission map with the luminance component of the haze image as the guidance image.

3. THE PROPOSED HAZE REMOVAL ALGORITHM

In this section, a new haze removal algorithm is proposed by introducing a minimal color channel and a non-negative sky region compensation term.

The model adopted to describe the formulation of a haze image is given as [1]

$$X_c(p) = \hat{Z}_c(p) t(p) + A_c(1 - t(p)), \quad (5)$$

where $c \in \{r, g, b\}$ is a color channel index, X_c is the observed intensity, $\hat{Z}_c$ is the scene radiance, A_c is the global atmospheric light, and t is the medium transmission describing the portion of the light that is not scattered and reaches the camera.

The first term $\hat{Z}_c(p)t(p)$ is called direct attenuation [5] and it describes the scene radiance and its decay in the medium. The second term $A_c(1 - t(p))$ is called airlight. Airlight results from previous scattered light and leads to the shift of the scene color. When the atmosphere is homogenous, the transmission $t(p)$ can be expressed as:

$$t(p) = e^{-\alpha d(p)}, \quad (6)$$

where α is the scattering coefficient of the atmosphere. It indicates that the scene radiance is attenuated exponentially with the scene depth $d(p)$. The value of α is a monotonically increasing function of the haze degree. When the haze becomes heavier, the term $A_c(1 - t(p))$ dominates the combination. As a result, the hazed image is smoother and the color fidelity of the hazed image is lost more. The objective of haze removal is to restore $\hat{Z}$ from the input X. Halo artifacts, amplification of noise in sky regions, and color fidelity are three major problems to be addressed for single image haze removal [12, 13].

Let $\Phi_c(\cdot)$ be a minimal operation along the color channel $\{r, g, b\}$. A_{min}, $X_{min}(p)$ and $\hat{Z}_{min}(p)$ are defined as

$$A_{min} = \Phi_c(A_c) = \min\{A_r, A_g, A_b\}, \quad (7)$$

$$X_{min}(p) = \Phi_c(X_c(p)) = \min\{X_r(p), X_g(p), X_b(p)\}, \quad (8)$$

$$\hat{Z}_{min}(p) = \Phi_c(\hat{Z}_c(p)) = \min\{\hat{Z}_r(p), \hat{Z}_g(p), \hat{Z}_b(p)\}. \quad (9)$$

X_{min} and $\hat{Z}_{min}$ are called the minimal color channels of the images X and $\hat{Z}$, respectively. It can be derived from the haze image model in Equation (5) that the relationship between the minimal color channels X_{min} and $\hat{Z}_{min}$ are given as

$$X_{min}(p) = \hat{Z}_{min}(p) t(p) + A_{min}(1 - t(p)). \quad (10)$$

Let $\Psi_\zeta(\cdot)$ be a minimal operation in the neighborhood $\Omega_\zeta(p)$ and it is defined as

$$\Psi_\zeta(z(p)) = \min_{p' \in \Omega_\zeta(p)} \{z(p')\}. \quad (11)$$

It is shown in [14] that the complexity of $\Psi_\zeta(\cdot)$ is $O(N)$ for an image with N pixels. A new dark channel is defined as

$$\hat{J}_{dark}^{\hat{Z}}(p) = \Psi_{\zeta_2}(\hat{Z}_{min}(p)), \quad (12)$$

where the value of ζ_2 is 7 in [7]. It is worth noting that the dark channel in [7] is defined as

$$J_{dark}^{\hat{Z}}(p) = \Phi_c(\Psi_{\zeta_2}(\hat{Z}_c(p))). \quad (13)$$

Three minimal operations $\Psi_{\zeta_2}(\cdot)$ and one minimal operation $\Phi_c(\cdot)$ are required to compute $J_{dark}^{\hat{Z}}(p)$ for the pixel p. With the new dark channel $\hat{J}_{dark}^{\hat{Z}}(p)$, only one minimal operations $\Psi_{\zeta_2}(\cdot)$ and one minimal operation $\Phi_c(\cdot)$ are required to compute the dark channel for the pixel p. Clearly, the computational cost of $\hat{J}_{dark}^{\hat{Z}}(p)$ is lower than that of $J_{dark}^{\hat{Z}}(p)$ even though the complexity of $\Psi_{\zeta_2}(\cdot)$ is $O(N)$ for an image with N pixels.

Similar to [7], we assume that the value of $t(p)$ is constant in the neighborhood $\Omega_{\zeta_2}(p)$. It can be derived from Equation (10) that

$$\hat{J}_{dark}^{X}(p) = \hat{J}_{dark}^{\hat{Z}}(p) t(p) + A_{min}(1 - t(p)). \quad (14)$$

Since $\hat{J}_{dark}^{\hat{Z}}(p) \approx 0$, the value of $t(p)$ can be initially estimated as

$$t(p) = 1 - \frac{\hat{J}_{dark}^{X}(p)}{A_{min}}. \quad (15)$$

It is worth noting that the initial value of $t(p)$ in [7] is given as

$$t(p) = 1 - \Phi_c(\Psi_{\zeta_2}(\frac{\hat{Z}_c(p)}{A_c})). \quad (16)$$

Obviously, it is simpler to estimate the initial value of $t(p)$ by using the proposed simplified dark channel.

The value of $A_c(c \in \{r, g, b\})$ is estimated by using $\hat{J}_{dark}^{X}(p)$ and $X_c(p)$. The brightest pixels in the dark channel are first selected. The value of $A_c(c \in \{r, g, b\})$ is set as the average inten-

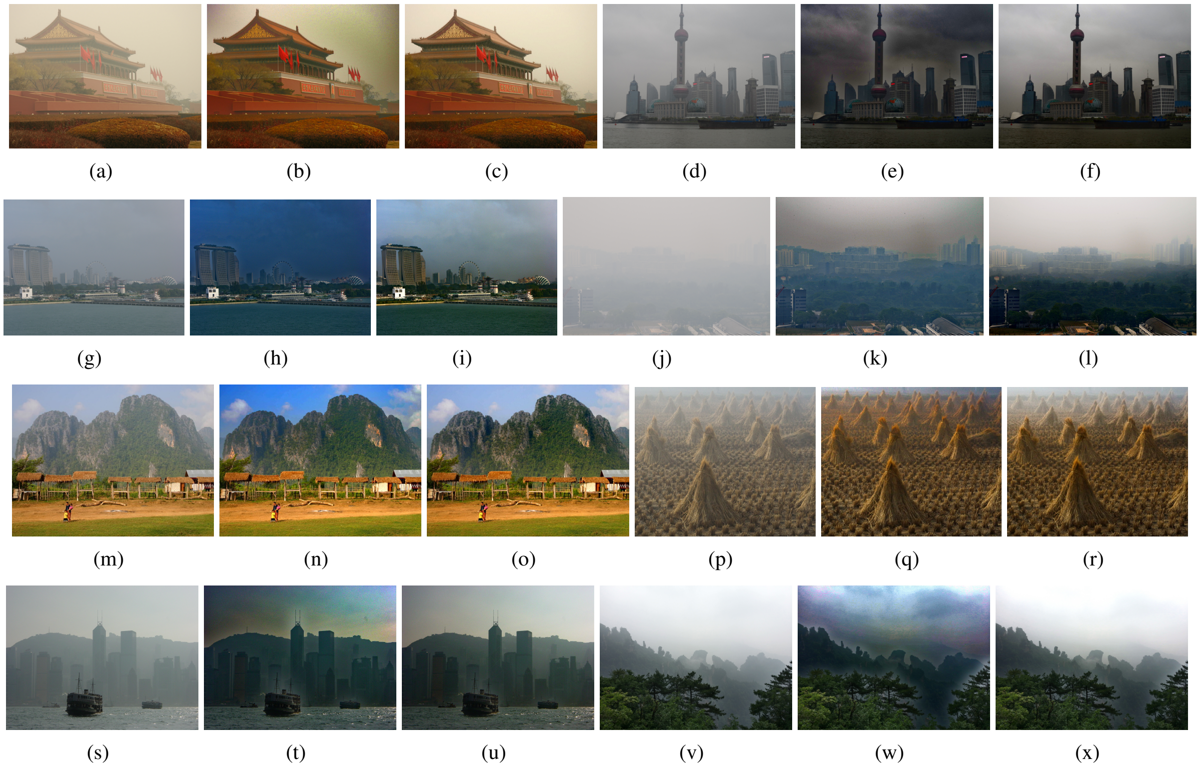

Fig. 1. Comparison of the proposed haze removal algorithm and the haze removal algorithm in [8]. (a, d, g, j, m, p, s, v) eight images with haze; (b, e, h, k, n, q, t, w) de-hazed images by the algorithm in [8]; (c, f, i, l, o, r, u, x) de-hazed images by the proposed algorithm.

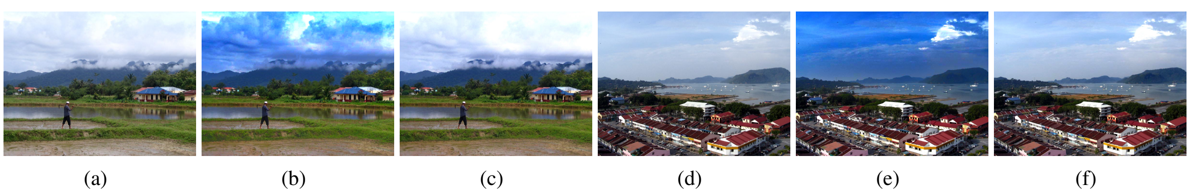

Fig. 2. Comparison of the proposed haze removal algorithm and the haze removal algorithm in [8] by using two sets of images without haze. (a, d) two images without haze; (b, e) de-hazed images by the algorithm in [8]; (c, f) de-hazed images by the proposed algorithm.

sity of these pixels along each color channel. The initial value of $t(p)$ is then computed as

$$t(p) = 1 - \frac{31}{32}\frac{\hat{J}^X_{dark}(p)}{A_{min}}. \tag{17}$$

The estimated transmission map $t(p)$ is then filtered by using the content adaptive GIF [11] with the guidance image as the luminance component of the haze image. The value of λ is set to 1/1000 as in [8, 13] and the value of ζ_1 to 60. The value of the transmission map $t(p)$ is further adjusted as

$$t(p) = t^{1+\theta}(p), \tag{18}$$

where the value of θ is adaptive to the haze level of the input image. Its value is 0/0.03125/0.0625 if the input image is with light/normal/heavy haze. Finally, the scene radiance $\hat{Z}(p)$ is recovered by

$$\hat{Z}_c(p) = (X_c(p) - A_c)/t(p) + A_c \; ; \; c \in \{r, g, b\}. \tag{19}$$

It can be derived that Equation (19) is equivalent to

$$\hat{Z}_c(p) = X_c(p) + (\frac{1}{t(p)} - 1)(X_c(p) - A_c). \tag{20}$$

It is shown in Equation (6) that the value of $t(p)$ is always less than or equal to 1, the single image haze removal thus can be regarded as a type of spatially varying detail enhancement. The detail layer is given as $(X_c(p) - A_c)$ and the amplification factor is $(\frac{1}{t(p)} - 1)$ which is spatially varying. Since the color of the sky is usually very similar to the atmospheric light A_c in a haze image, it can be shown that

$$\frac{\hat{J}^X_{dark}(p)}{A_{min}} \rightarrow 1, \text{and}, \frac{1}{t(p)} - 1 \rightarrow 31. \tag{21}$$

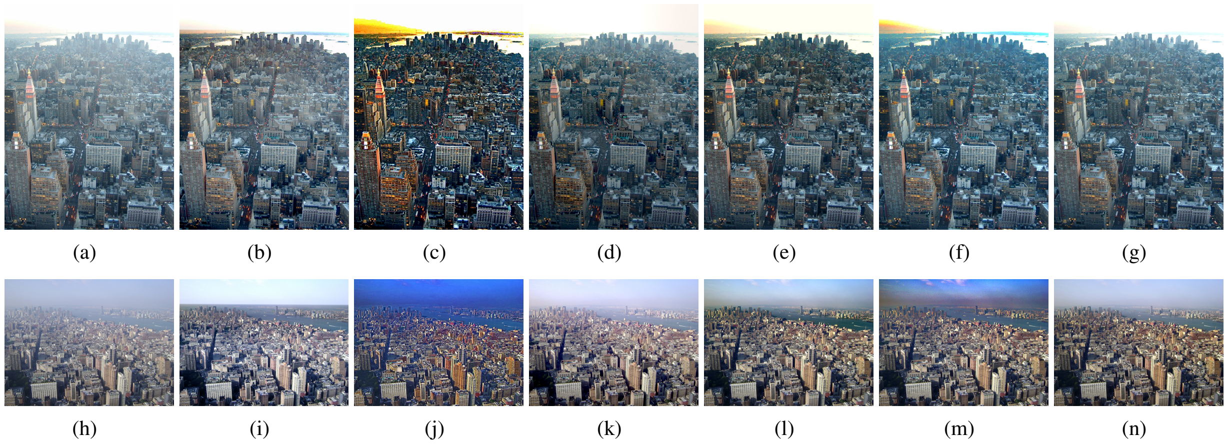

Fig. 3. Haze removal results by the algorithms in [4, 5, 6, 7, 8] and the proposed algorithm. (a, h) input images; (b, i) de-hazed images by the algorithm in [4]; (c, j) de-hazed images by the algorithm in [5]; (d, k) de-hazed images by the algorithm in [6]; (e, l) de-hazed images by the algorithm in [7]; (f, m) de-hazed images by the algorithm in [8]; and (g, n) de-hazed images by the proposed algorithm.

This implies that the value of the amplification factor is very large if the pixel p belongs to the sky region. A lower bound is pre-defined for the transmission map $t(p)$ in [7, 8] so as to limit the amplification factor. The lower bound is selected as 0.1 in [7, 8]. Similar to Equation (21), it can be computed that the the value of the amplification factors is about 9 if the pixel p belongs to the sky region. Experimental results in [7, 12] and in Fig. 1 show that noise could be amplified and/or halo artifacts could be produced due to the large amplification factors in the sky region. An intuitive method is to select a large lower bound. Unfortunately, a large lower bound will preserve too much haze in the final image.

A non-negative sky region compensation term is introduced to adjust the initial value of the transmission map $t(p)$ in the sky region according to the haze degree of the input image X_c. The haze degree can be automatically detected by using the histogram of the image X_c. With the proposed sky region compensation term, the amplification factors in the sky region are reduced. As such, halo artifacts can be reduced/avoided from appearing in the final image $\hat{Z}_c$, and amplification of noise can be limited in the sky region. On the other hand, a very small amount of haze is left for the distant objects. Fortunately, the presence of haze is a fundamental cue for human to perceive depth [15, 16]. Therefore, the left very small amount of haze for the distant objects helps preserve the feeling of depth in the dehazed image better as shown in Figs 1-3.

4. EXPERIMENTAL RESULTS

In this section, the proposed haze removal algorithm is compared with the haze removal algorithms in [4, 5, 6, 7, 8] by testing ten images with haze and two images without haze.

The proposed algorithm is first compared with the algorithm in [8] by testing eight images with haze. As can be seen from Fig. 1, the proposed algorithm neither has artifacts in sky regions nor halo artifacts as opposed to those from [8]. The running times of the proposed algorithm in the matlab code are respectively 0.8, 5.25, 13.7, 8.31, 0.63, 0.56, 5.25, and 8.69 seconds while those of the algorithm in [8] are respectively 0.86, 5.32, 13.62, 8.1, 0.72, 0.64, 5.28, 8.88 seconds. The speed of the proposed algorithm is comparable to the algorithm in [8]. The proposed algorithm is then compared with the algorithm in [8] by testing two images without haze. The two images without haze and their dehazed images are demonstrated in Fig. 2. The proposed algorithm introduces less color distortion than the algorithm in [8]. Clearly, the quality of the deahzed images by the proposed algorithm is much better than the quality of the dehazed images by the haze removal algorithm in [8].

The proposed algorithm is finally compared with the algorithms in [4, 5, 6, 7, 8] by testing two images with haze. As illustrated in Fig. 3, the images de-hazed by the proposed algorithm are very close to those using the algorithm in [6, 7]. The colors of the images dehazed by the algorithm in [5] is over saturated. 3D models and texture maps of the scene are required by the algorithm in [4]. The additional information could come from Google Earth or satellite images.

As indicated in [8], one of the key performance improvement in [8] is that the algorithm is much simpler compared to the algorithm in [7]. The running time of the GIF is about 40ms for a 600×400 image while 10 seconds using the matting Laplacian matrix as in [7]. Therefore, the proposed de-hazing algorithm has the similar fast speed feature like [8] and it has excellent visual quality of the global optimization based algorithm in [7].

5. CONCLUSION AND DISCUSSION

A new single image haze removal algorithm was proposed by introducing a minimal color channel. A simplified dark channel is computed by using the minimal color channel. The transmission map is first estimated by using the simplified dark channel. The map is then refined via a content adaptive guided image filter and is finally applied to recover the haze image. Experimental results demonstrate that the proposed algorithm outperforms existing single image haze removal algorithms from either the speed point of view or the image quality point of view. On the other hand, the proposed algorithm also has its own limitation. Particularly, the estimated transmission map is invalid when a large local region of a scene object is inherently similar to the airlight. The proposed algorithm could fail on extreme cases.

References

[1] S. G. Narasimhan and S. K. Nayar, "Chromatic framework for vision in bad weather," In *Proc. IEEE Conf. Computer Vision and Pattern Recognition (CVPR)*, 2000.

[2] S. G. Narasimhan and S. K. Nayar, "Contrast restoration of weather degraded images," IEEE Trans. on Pattern Analysis and Machine Learning, vol . 25, no. 6, pp. 713-724, Jun. 2003.

[3] S. Shwartz, E. Namer, and Y. Y. Schechner, "Blind haze separation," In *Proc. IEEE Conf. Computer Vision and Pattern Recognition (CVPR)*, pp. 19841991, 2006.

[4] J. Kopf, B. Neubert, B. Chen, M. Cohen, D. Cohen-Or, O. Deussen, M. Uyttendaele, and D. Lischinski, "Deep photo: model-based photograph enhancement and viewing," In *SIGGRAPH Asia*, 2008.

[5] R. Tan, "Visibility in bad weather from a single image," In *Proc. IEEE Conf. Computer Vision and Pattern Recognition (CVPR)*, 2008.

[6] R. Fattal, "Single image dehazing," In *SIGGRAPH*, pp. 1-9, 2008.

[7] K. He, J. Sun, and X. Tang, "Single image haze removal using dark channel prior," IEEE Trans. On Pattern Analysis and Machine Learning, vol. 33, no. 12, pp. 2341-2353, Dec 2011.

[8] K. He, J. Sun, and X. Tang, " Guided image filtering," IEEE Trans. On Pattern Analysis and Machine Learning, vol. 35, no. 6, pp. 1397-1409, Jun. 2013.

[9] C. Tomasi and R. Manduchi, "Bilateral filtering for gray and color images," In *Proc. IEEE Int. Conf. on Computer Vision*, pp. 836-846, 1998.

[10] Z. G. Li, J. H. Zheng, Z. J. Zhu, S. Q. Wu, W. Yao and S. Rahardja, "Content adaptive bilateral filtering," In *IEEE 2013 Int. Conf. on Multimedia and Expo*, Jul. 2013.

[11] Z. G. Li, J. H. Zheng, and Z. J. Zhu, "Content adaptive guided image filtering," In *IEEE 2014 Int.l Conf. on Multimedia and Expo*, paper 11, Jul. 2014.

[12] X. Y. Lv, W. Chen, and I. Shen, "Real-time dehazing for image and video," In *2010 18th Pacific Conf. on Computer Graphics and Applications*, pp. 62-69, Sep. 2010.

[13] J. H. Pang, O. C. Au, and Z. Guo, "Improved single image dehazing using guided filter," In *APSIPA ASC 2011*, pp. 1-4, China, 2011.

[14] M. van Herk, "A fast algorithm for local minimum and maximum filters on rectangular and octagonal kernels," Pattern Recogn. Lett., vol. 13, pp.517521, 1992.

[15] E. B. Goldstein, Sensation and perception. 1980.

[16] A. J. Preetham, P. Shirley, and B. Smits, "A practical analytic model for daylight," In *SIGGRAPH*, pp. 91100, 1999.

[17] F. J. Richards, "A flexible growth function for empirical use," Journal of Experimental Botany, vol. 10, no. 2, pp. 290-301, Feb. 1959.

[18] A. Zomet and S. Peleg, "Multi-sensor super resolution," In *Sixth IEEE Workshop on Applications of Computer Vision*, pp. 27-31, 2002.

[19] A. Torralba and W. T. Freeman, "Properties and applications of shape recipes," In *IEEE Computer Vision and Pattern Recognition*, pp. 383-390, 2003.

[20] A. Levin, D. Lischinski, and Y. Weiss, "A closed form solution to natural image matting," IEEE Trans. on Pattern Analysis and Machine Intelligence, vol. 30, no. 2, pp. 228-242, Feb. 2008.